

1 **Supplementary information for:**

2
3 **What controls the interannual variation of Hadley cell extent in the Northern**
4 **Hemisphere: Physical mechanism and empirical model for edge variation**

5
6
7 **Kyong-Hwan Seo** ^{1,2,3*}, **Sang-Pil Yoon**^{1,3}, **Jian Lu**⁴, **Yongyun Hu**⁵, **Paul W. Staten**^{6*}
8 **and Dargan M. W. Frierson**⁷

9
10 *¹Department of Atmospheric Sciences, Division of Earth Environmental System,*
11 *Pusan National University, Busan 46241, South Korea*

12 *²Research Center for Climate Sciences, Pusan National University, Busan 46241,*
13 *South Korea*

14 *³Future Earth Research Institute, PNU JYS Science Academy, Pusan National University,*
15 *Busan 46241, South Korea*

16 *⁴Pacific Northwest National Laboratory, Richmond, WA 99354, USA*

17 *⁵Department of Atmospheric and Oceanic Sciences, School of Physics, Peking University,*
18 *Beijing 100871, China*

19 *⁶Department of Earth and Atmospheric Sciences, Indiana University Bloomington,*
20 *Bloomington, IN 47405, USA*

21 *⁷Department of Atmospheric Sciences, University of Washington, Seattle, WA 98195, USA*

22

23

24 Contents of this file

25

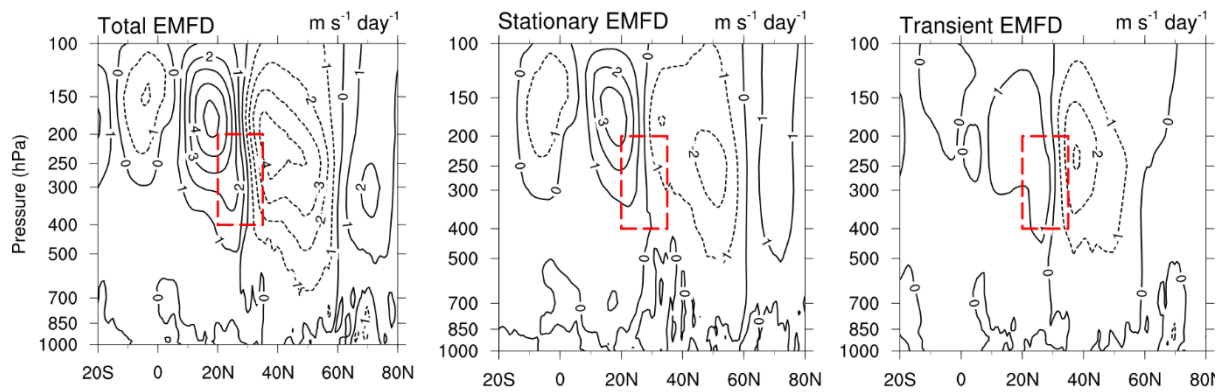
26 This supplementary material file has 9 figures.

27 Supplementary Figures 1 to 9

28

29

30



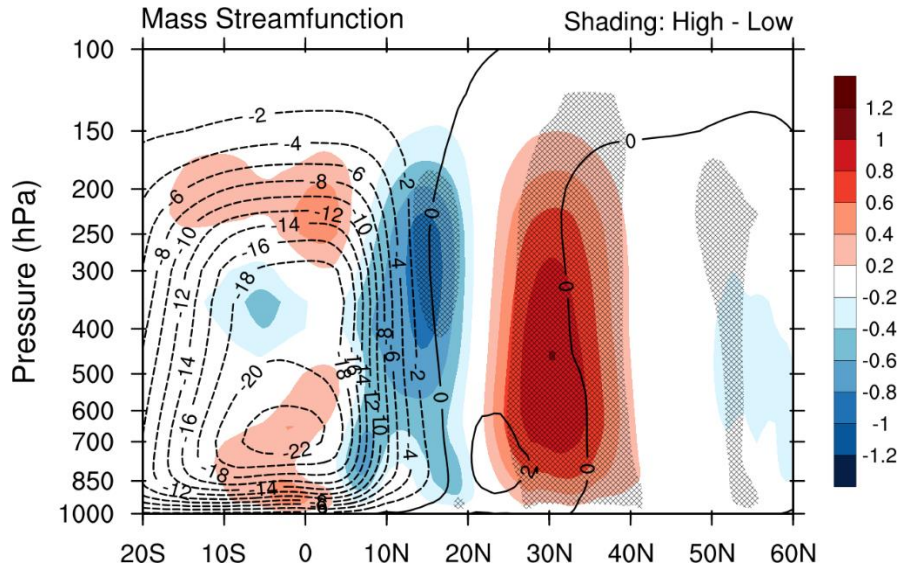
31

32 **Supplementary Figure 1. EMDF structure for DJFM.** Latitude–height plot of EMDF (in
33 units of $\text{m s}^{-1} \text{ day}^{-1}$) averaged over 41 years for (a) total wave, (b) stationary wave, and (c)
34 transient wave. Red box denotes a region enclosed by [400–200 hPa, 20°–35°N].

35

36

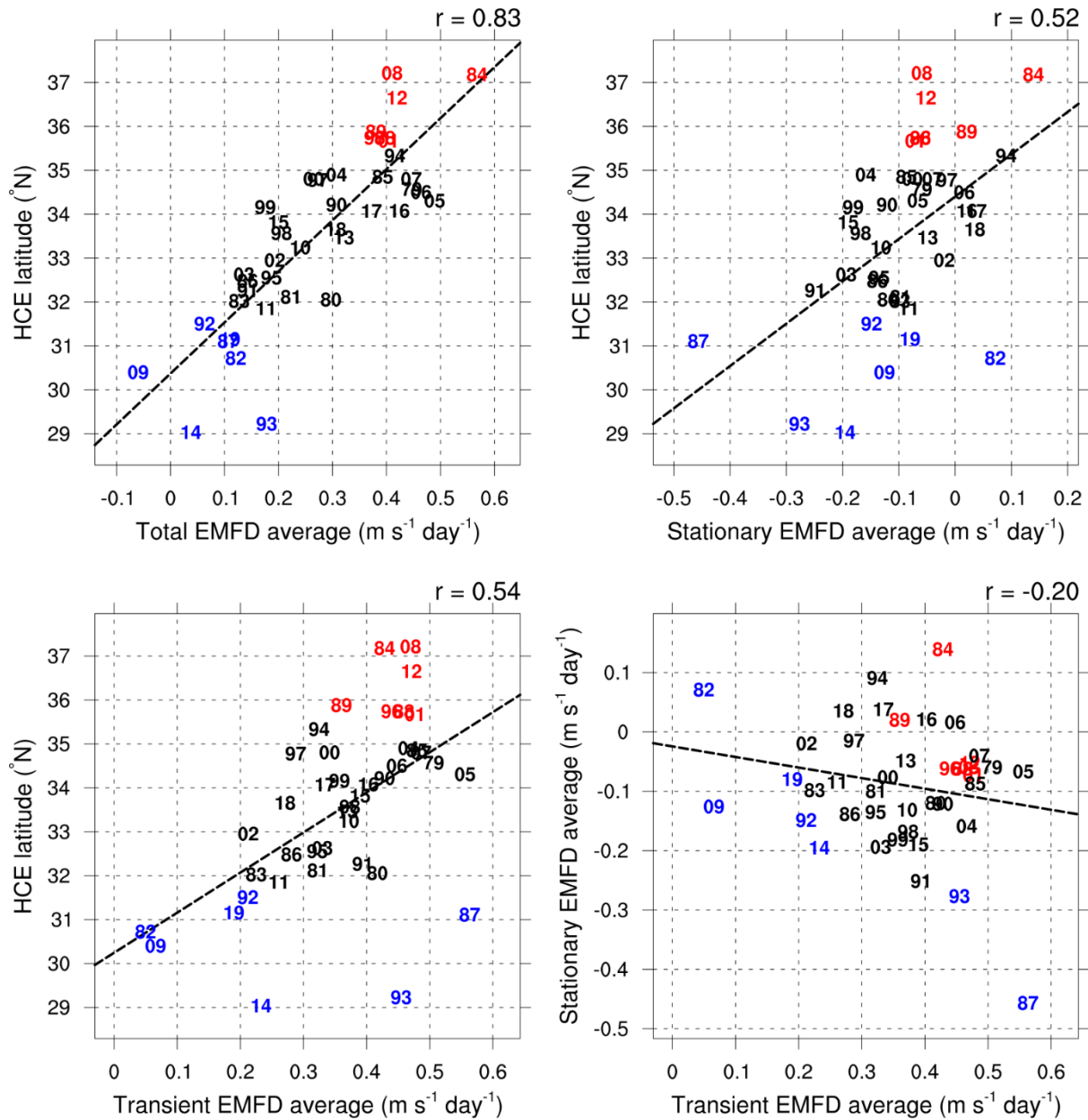
37



38

39 **Supplementary Figure 2. Streamfunction composite for JJAS.** Mass streamfunction for
 40 climatology (contour) and high-minus-low HCE latitude year composite (shading) for JJAS.
 41 Units are $10^{10} \text{ kg s}^{-1}$. Hatching denotes a significant area at the 95% confidence level.

42



43

44 **Supplementary Figure 3. Relationship between HCE latitude and EMFD for JJAS. (a)**

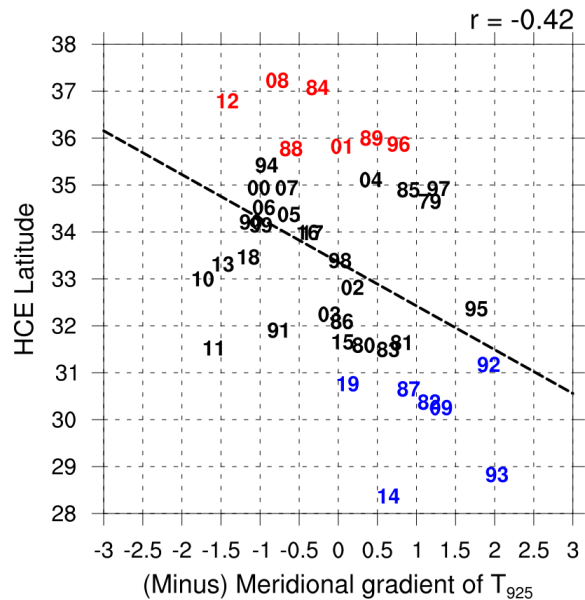
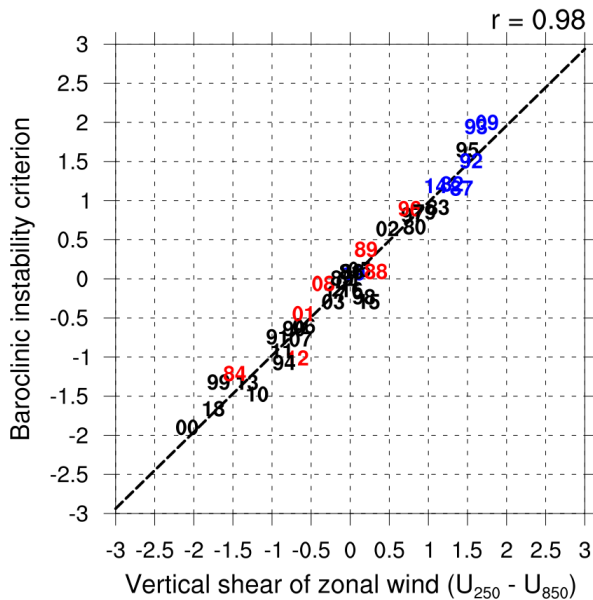
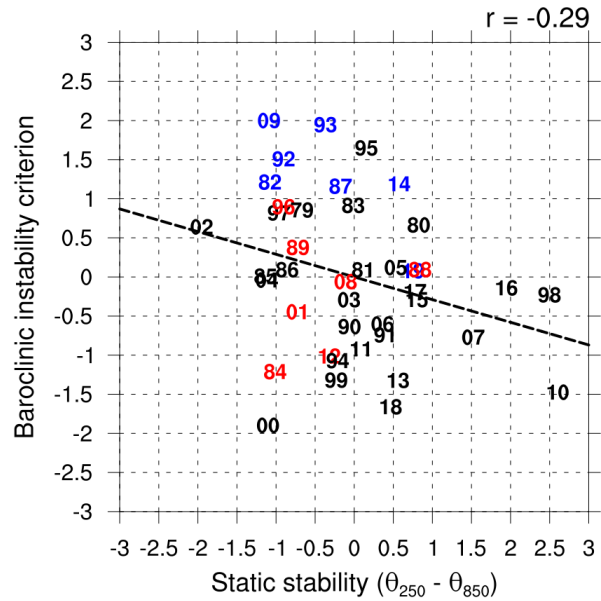
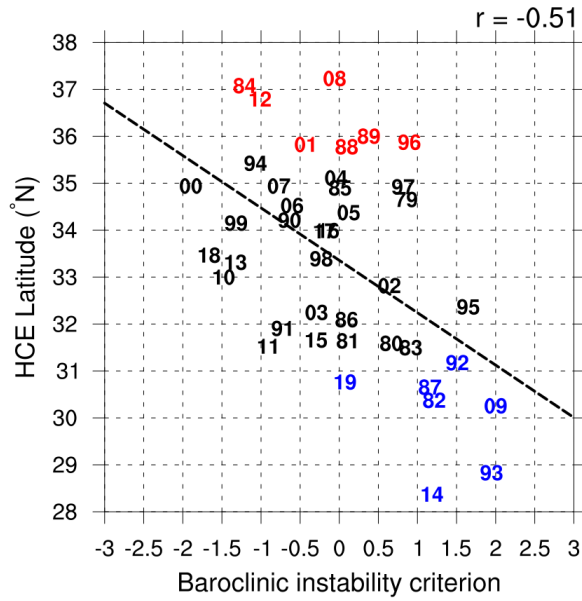
45 Scatter plot of (a) HCE latitude vs. EMFD averaged over a box enclosed by [400–200 hPa,

46 25°–40°N] for individual years during JJAS. The same as (a) except for (b) stationary wave

47 and (c) transient wave. (d) EMFD from stationary wave vs. that from transient wave. The

48 linear correlation is shown at the caption and linear regression lines are superimposed.

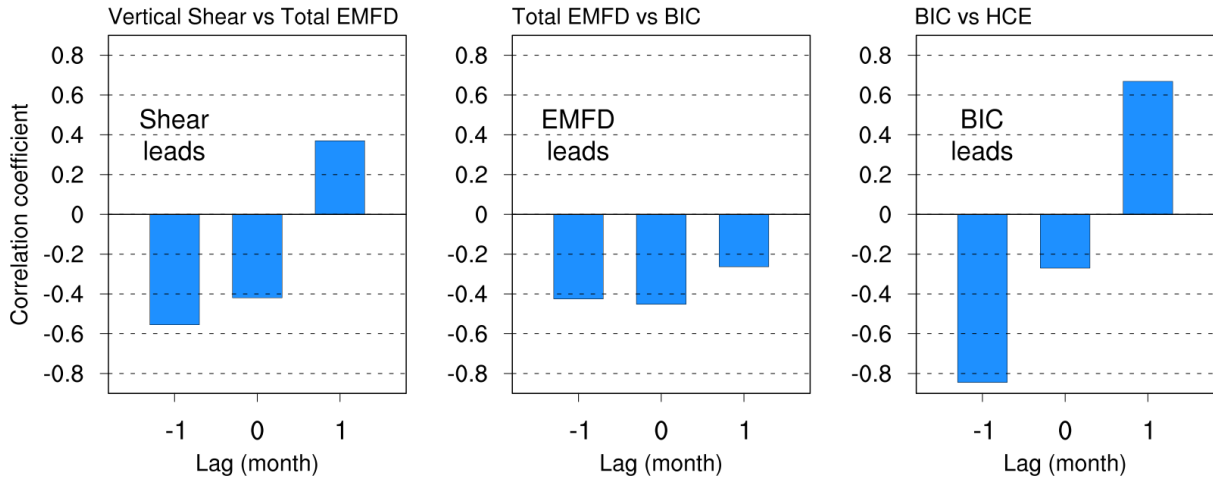
49



50
51
52
53
54
55
56
57
58

Supplementary Figure 4. Relationship between HCE latitude and baroclinicity for JJAS.

(a) BIC vs. HCE latitude ($^{\circ}\text{N}$), (b) bulk static stability (K) vs. BIC, (c) vertical wind shear (m s^{-1}) vs. BIC, and (d) (–)meridional temperature gradient at 925 hPa (K m^{-1}) vs. HCE latitude ($^{\circ}\text{N}$) for the latitudinal domain [25° – 40°N]. All variables have been standardized except for HCE latitude.

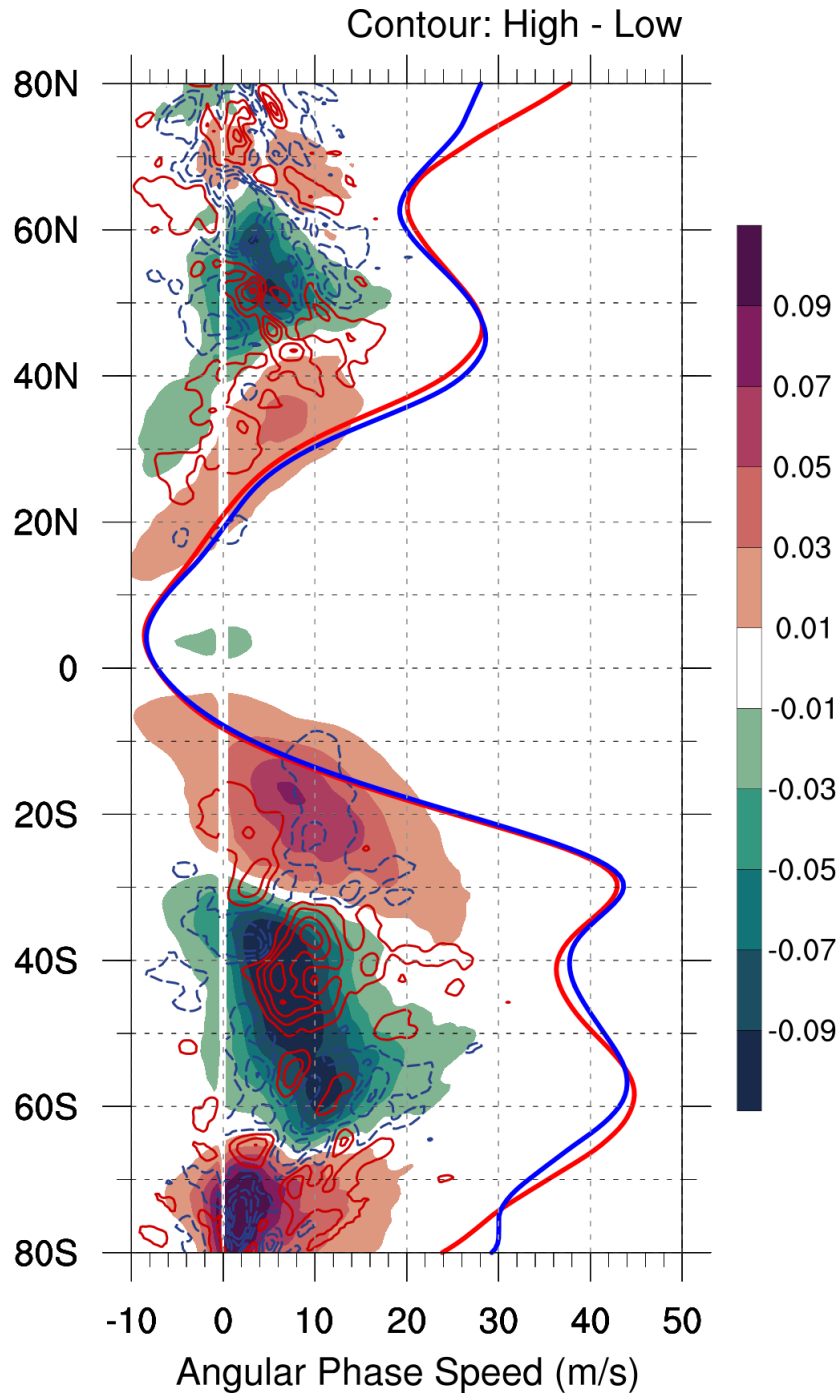


59

60 **Supplementary Figure 5. Temporal correlaton of related variables with HCE variation**

61 **for JJAS.** Lead–lag correlation coefficients between (a) vertical shear vs EMFD, (b) EMFD
 62 vs BIC (baroclinicity), and (c) BIC vs HCE, using DJFM monthly data. Averaged latitudinal
 63 domain is [25°–40°N].

64



65

66 **Supplementary Figure 6. Spectral analysis and application of critical latitude theory.**

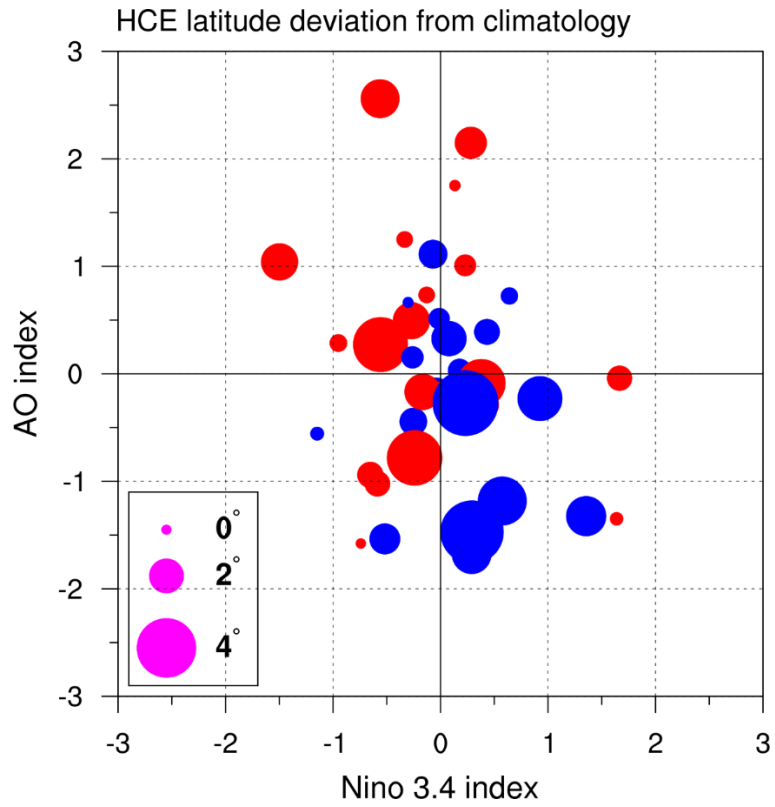
67 Co-spectrum ($\text{m s}^{-1} \text{ day}^{-1}$) of the EMFD at 250 hPa (red and blue contour, intervals of 0.01 m

68 $\text{s}^{-1} \text{ day}^{-1}$ with zero omitted) during JJAS for high-minus-low HCE latitude years with

69 climatology (shading, intervals of 0.02 $\text{m s}^{-1} \text{ day}^{-1}$). On the right side are the 250-hPa zonal

70 winds (m s^{-1}) divided by $\cos(\text{latitude})$ for high (red line) and low (blue) HCE years.

71



72

73 **Supplementary Figure 7. HCE latitude as a function of two natural variabilities during**

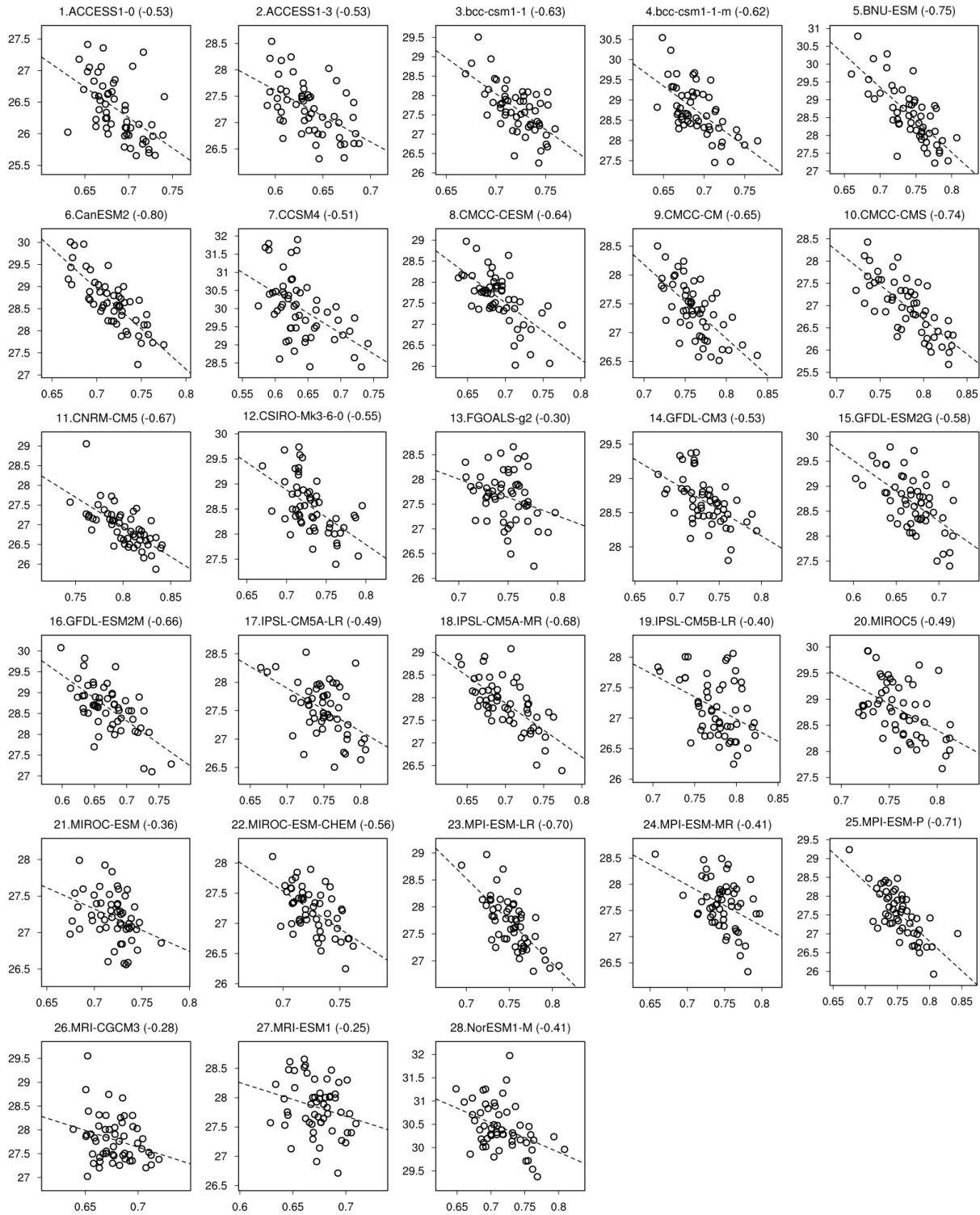
74 **JJAS.** Scatter plot of HCE latitude deviation from mean with respect to the axes of NIÑO3.4

75 and AO indices for 41-year data during JJAS. Positive (negative) deviations are in red (blue)

76 dots with their size representing the magnitude of HCE latitude deviation.

77

78



79

80

Supplementary Figure 8. Validation using CMIP5 data for DJFM. Scatter plot of BIC

81

(abscissa) averaged over $[20^{\circ}-35^{\circ}\text{N}]$ vs. HCE latitude ($^{\circ}\text{N}$, ordinate) for the period from 1950

82

to 2005 (55 DJFMs) for 28 CMIP5 models. Among these, 12 models (3, 4, 5, 6, 8, 9, 10, 11,

83

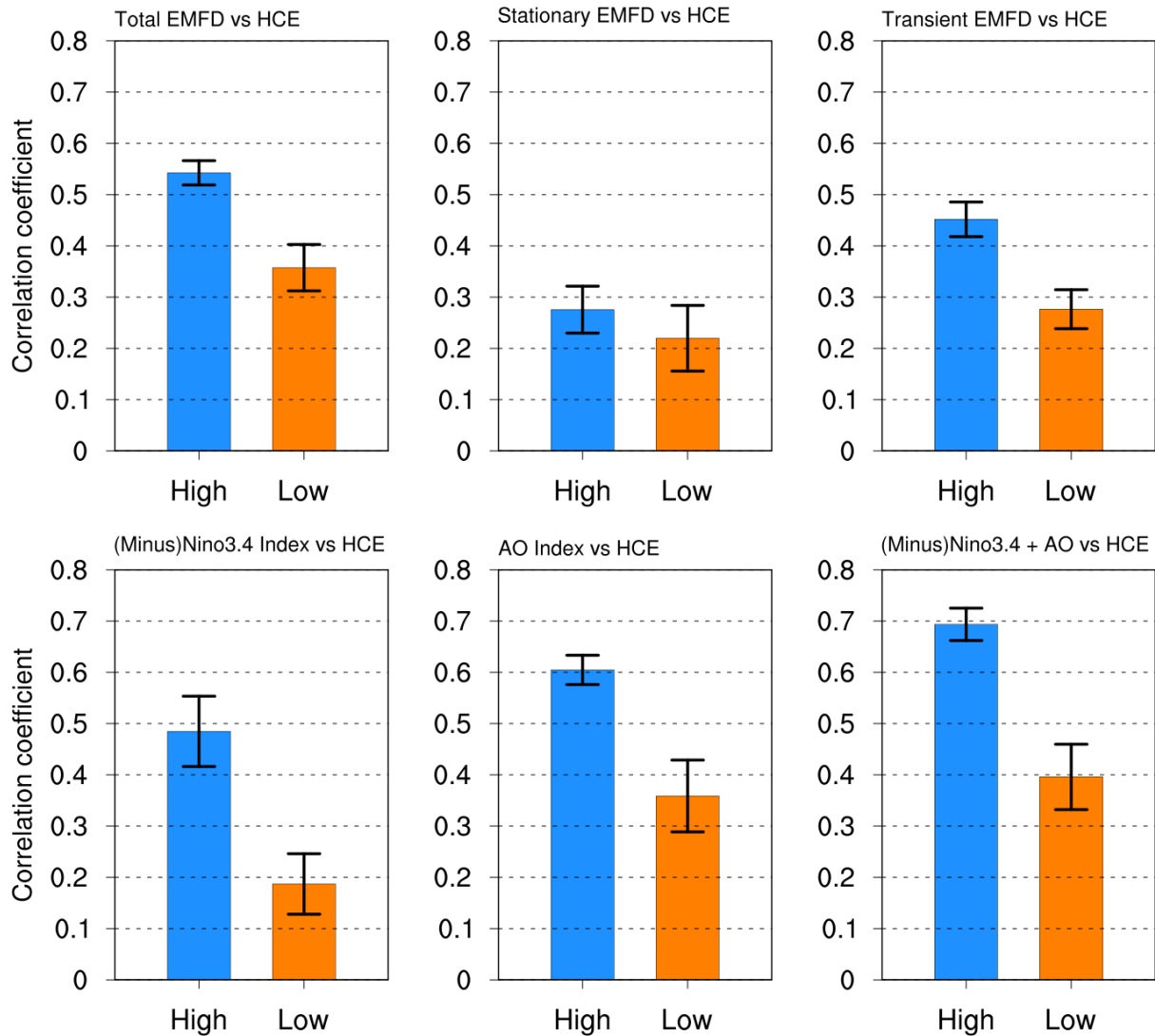
16, 18, 23, and 25) are selected as the high correlation model group, whereas 9 models (13,

84

17, 19, 20, 21, 24, 26, 27, and 28) are as the low correlation model group. The correlation

85

coefficient is presented in the caption of each panel.



86
 87 **Supplementary Figure 9. Validation using CMIP5 two select groups for DJFM.** Average
 88 correlation coefficient between HCE latitude and (a) total, (b) stationary, and (c) transient
 89 EMFD during DJFM for 10 high correlation and 8 low correlation model groups. EMFD is
 90 calculated for the domain [400–200 hPa, 20°–35°N], as shown in Supplementary Figure 1.
 91 Average correlation coefficients (d) between HCE latitude and (–)NIÑO3.4 index, (e)
 92 between HCE latitude and AO index, and (f) between HCE latitude and combined index
 93 using (–)NIÑO3.4+AO. Error bar represents standard error.

94